# Measurement of the Size Dependent Hole Spectrum in CdSe Quantum Dots

D. J. Norris, A. Sacra, C. B. Murray, and M. G. Bawendi
*Massachusetts Institute of Technology, 77 Massachusetts Avenue, Cambridge, Massachusetts 02139*

(Received 1 July 1993)

We combine a new synthesis with transient optical hole burning to observe and assign the size evolution (19 to 115 Å diameter, $\sigma < 5\%$) of a series of excited states in CdSe quantum dots. We observe an avoided crossing around the spin orbit energy in the hole spectra for ~65 Å dots, indicating the importance of valence band complexities in the description of the excited states. Comparison with dc Stark data shows that bleach spectra are consistent with localized carrier induced electric fields.

PACS numbers: 73.20.Dx, 36.40.+d, 73.20.At, 73.20.Fz

Nanometer size structures provide the opportunity to observe and control the properties of materials as they evolve from molecules to the bulk. In particular, semiconductor electronic transitions show interesting and strongly size dependent properties in this size regime. Nanometer size semiconductor crystallites (quantum dots) which are small compared to the bulk exciton Bohr radius exhibit three dimensional quantum confinement [1]. Quantum dots, often called "artificial atoms," possess in principle discrete electronic excitations with wave functions delocalized within and confined by the dot boundary. Numerous studies [1-9] have probed the lowest photoexcited state in II-VI dots. Its confinement induced shift to higher energy with decreasing diameter is well established [1]. However, experimental investigation of the size evolution of the higher excited states has been difficult. The discrete nature of these states is usually concealed by sample inhomogeneities such as distributions in size, shape, and stoichiometry.

The observation and assignment of a series of excited states in CdSe quantum dots, the variation of their spacings with size, and the comparison of these spacings with recent theory are the focus of this Letter. Our ability to observe a series of excited states depends crucially on a recently developed synthesis which provides II-VI quantum dots with a high degree of monodispersity (< 5% rms), consistent crystal structure and surface derivatization, and control of size from ~12 to ~115 Å in diameter [9]. Unlike most samples prepared in silicate glasses and previous samples in polymer films which typically emit from deep trap states with low quantum yield, our samples show "band edge" luminescence with little deep trap emission and high quantum yield (ranging from 0.1 to 0.9 at 10 K). The high quality of our samples is demonstrated in Fig. 1(a) by the absorption spectra of a series of sizes from 19 to 115 Å in diameter. As many as six transitions can be resolved in a single sample.

Although this sample series represents the highest quality yet reported, the main contribution to the width of the absorption features remains sample inhomogeneities. Nanosecond pump-probe spectroscopy can further resolve the transitions [2-5]. With this technique we optically select a subset of the quantum dot size distribution by exciting each sample on the red edge of its first transition with a spectrally narrow pump beam. The pump-induced change in optical density (OD) contains both bleached and induced absorptions arising from particles already containing an electron-hole pair [Fig. 1(b)]. Comparison of pump-probe spectra [Fig. 1(b)] with absorption data [Fig. 1(a)] shows that bleached features correspond to ground state transitions, but are more clearly resolved. To independently verify this conclusion we use another size-selective technique, photoluminescence excitation (PLE). PLE reveals the positions of ground state absorptions by measuring luminescence intensity as a function of excitation energy. To measure only a subset of the size distribution, we monitor a narrow spectral band on the blue edge of the full luminescence while scanning the excitation wavelength [3]. Our PLE results [Figs. 1(c) and 1(d)] clearly confirm that pump-probe bleaches lie at the positions of ground state transitions.

Pump-probe spectra for our entire series of dots is shown in Fig. 2. This series spans the strong confinement regime in which electron-hole Coulomb interactions are much smaller than the confinement energies. This situation is addressed in early theoretical work by combining a simple two band isotropic effective mass model with a spherical boundary condition and treating the electron and hole separately [1]. The wave functions are described by "particle-in-a-sphere" envelope functions with electron and hole angular momenta $L_e$ and $L_h$. However, this approach ignores the complexities of the CdSe valence band which is formed from Se $p$ atomic orbitals. The sixfold degenerate valence band is split by spin-orbit coupling into a band-edge fourfold degenerate $J=3/2$ band and a twofold degenerate $J=1/2$ band. For dot hole levels arising from these bands the envelope function angular momentum, $L_h$, and the unit cell angular momentum, $J$, are not good quantum numbers. Only the total angular momentum, $F=L_h+J$, and parity are conserved. States with the same $F$ and equal parity mix [10,11]. Therefore, each hole level with total momentum $F$ (labeled as $n_hL_F$) is a mixture of $L_h$ and $L_h+2$ envelope functions. The electron states, not affected by the valence band complications, are labeled as $n_eL_e$. [$n_{h(e)}$

0031-9007/94/72(16)/2612(4)$06.00

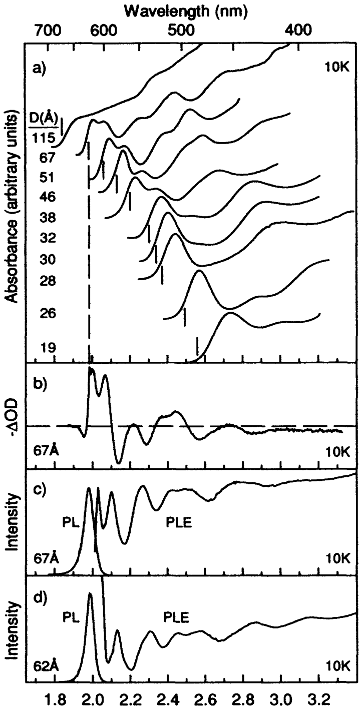

FIG. 1. (a) Absorption spectra (10 K) for CdSe dots embedded in optically clear poly(vinyl butyral) (PVB) films (offset for clarity). Typical OD at the first absorption feature is 0.3–0.6. Mean diameters are measured by TEM. Black vertical lines mark pump frequencies. (b) Bleach spectrum, plotted as negative change in optical density, for 67 Å dots (10 K). Positive (negative) peaks are bleaches (induced absorptions). The dashed horizontal line represents $-\Delta OD = 0$. A 10 Hz $Q$-switched Nd:YAG/dye laser system (~7 ns pulses) produced both pump (1.984 eV) and spectrally broad probe pulses, separated by 12 ns. (To measure bleach lifetime, a second synchronized 10 Hz $Q$-switched Nd:YAG laser produced delayed probe pulses.) Pump intensity ($< 100$ kW/cm$^2$) was controlled to ensure linear absorption, checked via luminescence. Transmitted probe light was dispersed and detected with a 5 ns gated optical multichannel analyzer. (c) Fluorescence and PLE spectra for 67 Å dots (10 K). Emission for PLE was observed at 2.016 eV with a ~1.5 meV bandpass. A small energy shift (utilized in Fig. 3) exists between the pump-probe and PLE spectra since the two techniques sample different portions of the size distribution. (d) Fluorescence and PLE spectra for ~62 Å dots (10 K). Emission for PLE observed at 2.022 eV with a ~0.7 meV bandpass.

are counters which number hole (electron) eigenstates for a given symmetry.] For example, the first excited state is written as $1S_{3/2}1S_e$, which contains contributions from the following hole states: $(J=3/2,\ L_h=0,\ F=3/2)$, $(J=3/2,\ L_h=2,\ F=3/2)$, and from the split off band $(J=1/2,\ L_h=2,\ F=3/2)$. Within the strong confinement approximation, the Coulomb effect is added as a first order perturbation. In reality, especially for the larger dots, the Coulomb interaction further mixes these eigenstates and alters oscillator strengths [12].

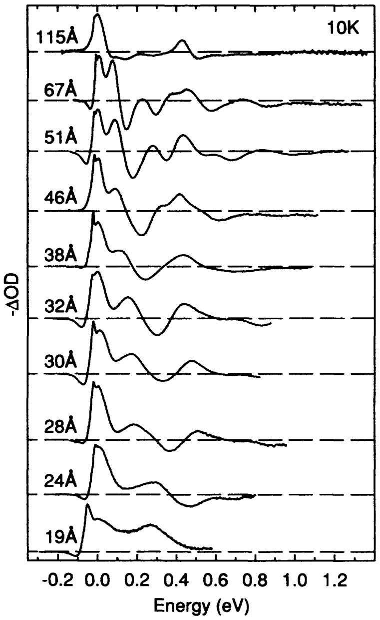

FIG. 2. Bleach spectra (10 K), with pump energies: 1.842, 1.984, 2.060, 2.130, 2.198, 2.296, 2.339, 2.366, 2.490, and 2.557 eV for 115 to 19 Å dots. $1S_{3/2}1S_e$ transitions, typically bleached several percent, are set to zero energy.

From Fig. 2 we extract the bleached absorption positions by fitting the spectra to a sum of positive- (bleaches) and negative-going (induced absorptions) Gaussians by standard least squares methods. Since some spectra are difficult to interpret due to overlap of bleaches with induced absorptions we assign only those features which can be followed through several sizes. Questionable peaks close to the zero crossing, such as the broad plateau at 0.7 eV for 32 and 30 Å dots, are not included. When we compare our results with theory, we find that, as with simpler models, even the recent sophisticated effective mass theory of Ref. [11], which includes spin-orbit coupling, valence band degeneracies, and the nonparabolicity of the conduction band, increasingly overestimates the confinement energy with decreasing size. This theory diverges in part due to its assumption of an infinite potential barrier at the dot boundary, but also due to the failure in general of effective mass theory for the smallest dots, which are better described in more molecular terms [1,11,13]. Most of the theoretical error originates in predicting the electron level ($m_e \ll m_h$). Since most of the lowest allowed transitions contain the same electron level ($1S_e$), plotting transition energies relative to the first excited state ($1S_{3/2}1S_e$) minimizes the theoretical deviation in comparisons of theory with experimental results. Such a plot removes the common and problematic electron contribution and yields the hole spectrum in CdSe quantum dots.

Figure 3 (solid squares) shows our observed excited

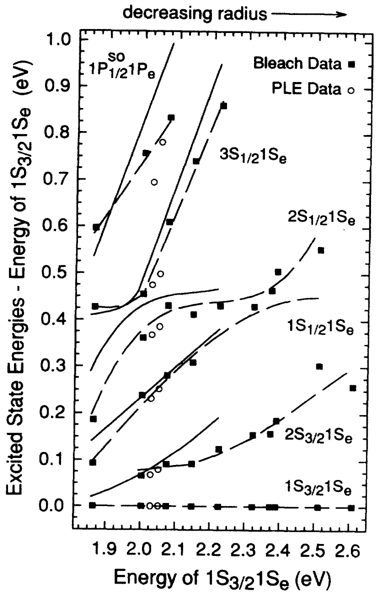

FIG. 3. Excited state spacings from Fig. 2 (solid squares), plotted relative to $1S_{3/2}1S_e$. The $x$ axis is the size dependent energy of $1S_{3/2}1S_e$. Dashed lines are visual guides for our assignments. Solid lines are predictions from Fig. 3 of Ref. [11(b)]. PLE data from Figs. 1(c) and 1(d) are plotted (open circles) to further support the observation of an avoided crossing.

state energy spacings (relative to $1S_{3/2}1S_e$) as a function of the energy of the $1S_{3/2}1S_e$ state. We use this $x$ axis instead of dot diameter since the energy of the $1S_{3/2}1S_e$ state is experimentally more precisely measured than dot size. Using size would introduce significant noise to the plot due to measurement errors. In addition, the diameters quoted in Fig. 1 are mean values which do not address the subset of the size distribution measured in the bleach results. Instead, we use the energy of the $1S_{3/2}1S_e$ state, which is easily and accurately determined and is a better size dependent label for those dots that are actually probed. The dashed lines in Fig. 3, visual guides for our assignments, trace the evolution of observed transitions with size. The solid lines are the prediction of Ref. [11]. We do not plot theoretical curves for all allowed transitions, but rather those which best fit the experimental results. Our assignments are based on the good agreement between data and theory. Surprisingly, we do not observe several transitions expected to be strongly allowed, e.g., $1P_{3/2}1P_e$ [11]. However, these transitions, as with other unobserved allowed transitions, poorly match the experimental points in Fig. 3, both in position and slope. These transitions may be hidden by strong induced absorptions in the pump-probe data.

We stress that simple effective mass theory cannot account for our data. A series of states split from $1S_{3/2}1S_e$ by spin-orbit coupling (0.42 eV) is seen in Fig. 3. These states, which evolve into the bulk spin-orbit band ($C$ band), appear in zeroth order theory as a horizontal line due to the similar effective masses of the bulk $A$ and $C$ bands. In reality this series of states is perturbed by nearby hole eigenstates with the same symmetry. We observe this situation in the bleach data as the avoided crossing of the $2S_{1/2}1S_e$ and $3S_{1/2}1S_e$ states for ~65 Å dots. To confirm this claim we plot PLE data from Figs. 1(c) and 1(d) at the crossing region in Fig. 3 (open circles). The avoided crossing is intimately connected with the mixture of $L_h$ and $L_h+2$ envelope functions in the hole eigenstates and, therefore, it is instructive to focus on the $2S_{1/2}1S_e$ state in Figs. 2 and 3 and follow the change in its $L_h$ and $L_h+2$ components as a function of size. This state is a mixture of $d$-like ($J=3/2$, $L_h=2$, $F=1/2$) and $s$-like ($J=1/2$, $L_h=0$, $F=1/2$) hole levels only. All of the oscillator strength comes from the $s$-like component which couples strongly to the $1S_e$ electron level. In large dots, the $2S_{1/2}1S_e$ state has the hole mostly in the $d$-like $J=3/2$ level, and is a weak transition. After the avoided crossing with the $3S_{1/2}1S_e$ state, the hole state becomes mostly $s$-like from the $J=1/2$ band and gains oscillator strength. This variation in absorption strength is observed in Fig. 2 and provides additional evidence for our assignments. In small dots, the hole returns to weakly absorbing $d$-like character ($J=3/2$) after the avoided crossing with the $1S_{1/2}1S_e$ state. Unfortunately, the avoided crossing of the $1S_{1/2}1S_e$ and $2S_{1/2}1S_e$ states at ~32 Å is not observed, probably due to overlap with strong induced absorptions.

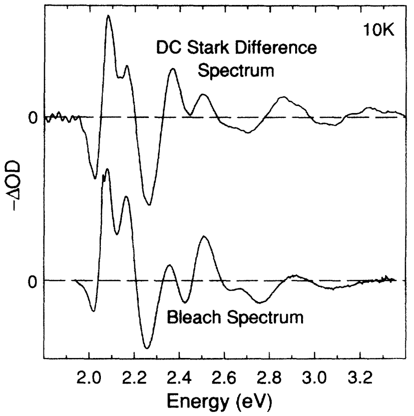

FIG. 4. dc Stark difference (field on-field off, $\sim 5\times10^4$ V/cm internal field, 10 K) and bleach spectra for 51 Å CdSe dots. With this field and pump power close to saturation the bleach signal is ~4× larger than the Stark signal for similar optical densities. For the pump-probe data, if we crudely model the dot as a delocalized electron with a "trapped," point source hole at the dot surface, we estimate that the electric field at the dot center is $2\times10^5$ V/cm. This very roughly implies one-fourth of the particles are excited, consistent with the experimental data.

To understand the origin of the pump-probe spectrum, Fig. 4 compares it with dc Stark data. The strong similarity seems to imply a common mechanism. The long lifetime of our pump-probe spectra (there is still signal after 10 $\mu$s) suggests that one or both of the excited carriers is localized in trap states. We argue that the electric field produced by separation of the first electron-hole pair causes a "Stark effect" on the absorption of a second pair [6]. Both shallow hole surface traps, observed in band edge luminescence studies [3,8] with a 100 ns-1 $\mu$s decay time, as well as longer lived ($> 1$ $\mu$s) weakly radiative or nonradiative deep trap states, contribute. In general a Stark field induces both a shift of state positions and a redistribution of oscillator strength. In the small field limit with well separated line shapes the Stark difference spectrum is proportional to the first derivative of the absorption spectrum, i.e., $\Delta\mathrm{OD}(\varepsilon) \propto E^2 f'(\varepsilon)$, where $E$ is the electric field, $f$ is the absorption line shape, and $\varepsilon$ is energy. This result can easily be shown by expressing the line shape as a Taylor expansion in the Stark shift and calculating the perturbing Stark interaction to second order. However, in the small field limit with broad absorption linewidths, larger than both the field induced shift and the separation between interacting states, the Stark difference spectrum is proportional to the second derivative of the absorption spectrum, or $\Delta\mathrm{OD}(\varepsilon) \propto E^2 f''(\varepsilon)$. This results from expressing the line shape in a Taylor expansion in both the Stark shift and the spacing between interacting states. In the limit of broad linewidths, the second derivative line shape implies that Stark bleaches appear at the positions of ground state transitions. The observable effect of the field is to bleach initially allowed transitions and cause induced absorptions due to both shifting lines and initially forbidden transitions gaining oscillator strength. This limit is appropriate for our system in which the interacting levels are closely spaced relative to the linewidths (for example, a forbidden $p$-like hole state lies in between the first two observed transitions [11]) and this description agrees with experiment. In the Stark difference spectra, we observe bleaches at the positions of the absorption peaks, as seen previously [14,15]. These bleaches show no field dependent shift but increase quadratically in magnitude with the field. Therefore, pump-probe bleaches in Fig. 2, which appear at the positions of ground state transitions, are consistent with a trapped carrier induced Stark effect.

It is surprising that the first excited state bleaches are so broad in our results. Pump-probe or PLE should considerably narrow the size distribution. The single particle $1S_{3/2}1S_e$ linewidth, determined from previous pump-probe and fluorescence line narrowing experiments [2,3,5,7], is significantly narrower (from 4 to 16 meV, increasing with decreasing size) [7]. We believe that the combination of a sharp bleach "spike" at the pump frequency and a broad bleach to the blue in each of our pump-probe spectra (Fig. 2) suggests an explanation. This structure is consistent with the existence of an absorption "tail" on the single particle $1S_{3/2}1S_e$ linewidth. This tail, which will be discussed in a separate publication, partially reintroduces the size distribution.

This Letter presents a measurement of the size dependence of a series of transitions in CdSe quantum dots. Good agreement with recent theoretical predictions allows us to assign the transitions. Our data show that the complexity of the valence band and the strong spin-orbit coupling in CdSe dominate the size dependence of excited state spacings. This is evident from the observation of an avoided crossing for ~65 Å quantum dots, observed in pump-probe spectra and confirmed by PLE. The strong similarity between the full bleach spectrum and dc Stark data suggests that electric fields produced by carrier localization induce a Stark effect in excited quantum dots.

We thank Al. L. Efros for stimulating discussions. D.J.N. and C.B.M. benefited from NSF and NSERC fellowships, respectively. This work was funded in part by the MIT Center for Materials Science and Engineering (NSF-DMR-90-22933), by NSF (DMR-91-57491, CHE-89-14953, ECS-91-18907), and by the Lucille and David Packard Foundation.

---

[1] Al. L. Efros and A. L. Efros, Fiz. Tekh. Poluprovodn. **16**, 1209 (1982) [Sov. Phys. Semicond. **16**, 772 (1982)]; L. E. Brus, J. Chem. Phys. **80**, 4403 (1984).

[2] A. P. Alivisatos, A. L. Harris, N. J. Levinos, M. L. Steigerwald, and L. E. Brus, J. Chem. Phys. **89**, 4001 (1988).

[3] M. G. Bawendi, W. L. Wilson, L. Rothberg, P. J. Carroll, T. M. Jedju, M. L. Steigerwald, and L. E. Brus, Phys. Rev. Lett. **65**, 1623 (1990); M. G. Bawendi, P. J. Carroll, W. L. Wilson, and L. E. Brus, J. Chem. Phys. **96**, 946 (1992).

[4] N. Peyghambarian *et al.*, IEEE J. Quantum Electron. **25**, 2516 (1989).

[5] U. Woggon, S. Gaponenko, W. Langbein, A. Uhrig, and C. Klingshirn, Phys. Rev. B **47**, 3684 (1983).

[6] E. F. Hilinski, P. A. Lucas, and Y. Wang, J. Chem. Phys. **89**, 3435 (1988).

[7] D. J. Norris, M. Nirmal, C. B. Murray, A. Sacra, and M. G. Bawendi, Z. Phys. D **26**, 355 (1993).

[8] M. O'Neil, J. Marohn, and G. McLendon, J. Phys. Chem. **94**, 4356 (1990); A. Eychmüller, A. Hässelbarth, L. Katsikas, and H. Weller, Ber. Bunsenges. Phys. Chem. **95**, 79 (1991).

[9] C. B. Murray, D. J. Norris, and M. G. Bawendi, J. Am. Chem. Soc. **115**, 8706 (1993).

[10] J. B. Xia, Phys. Rev. B **40**, 8500 (1989).

[11] (a) G. B. Grigoryan, E. M. Kazaryan, Al. L. Efros, and T. V. Yazeva, Sov. Phys. Solid State **32**, 1031 (1990); (b) A. I. Ekimov *et al.*, J. Opt. Soc. Am. B **10**, 100 (1993).

[12] Y. Z. Hu, M. Lindberg, and S. W. Koch, Phys. Rev. B **42**, 1713 (1990).

[13] Y. Wang and N. Herron, Phys. Rev. B **42**, 7253 (1990).

[14] F. Hache, D. Ricard, and C. Flytzanis, Appl. Phys. Lett. **55**, 1504 (1989).

[15] V. L. Colvin and A. P. Alivisatos, J. Chem. Phys. **97**, 730 (1992).